Optical Properties of the Phosphorescent Trinuclear Copper(I) Complexes of Pyrazolates: Insights from Theory

Bo Hu,[†,‡] Godefroid Gahungu,[†] and Jingping Zhang*[,†]

Faculty of Chemistry, Northeast Normal University, Changchun 130024, China, and Faculty of Chemistry, Jilin Normal University, Siping 136000, China

Received: December 25, 2006; In Final Form: April 11, 2007

Theoretical investigations have been performed to explore the optical properties of $\{[3,5\text{-}(CF_3)_2Pz]Cu\}_3$ in monomeric and dimeric forms using TD−DFT approaches. The emission of all complexes originates from the lowest triplet excited-states (T_1), and the corresponding emissive states are assigned as the mixture of the metal-centered charge transfer and ligand-to-metal charge transfer. The features of the emission spectrum are clarified in detail. The bulk emission spectrum of complex is mainly determined by the stacked dimers rather than the individual monomers. The predicted maximum emission wavelength (λ_{em}) are in good agreement with experimental values, indicating that the phosphorescence bands can be assigned to two different conformations for the neighboring stacked dimers sharing the same monomer in the complex. Energy transfer from T_1 of one stacked dimer to the neighboring one is responsible for the disappearance of the shoulder, leaving only the main peak upon heating. With the aim to reveal the conformational dependence for the triplet excited-state emission spectrum, the optical properties of various stacked dimers with different conformations are investigated by varying the relative arrangements through changing inter-monomer distance or rotational angles for the dimer which is responsible for the main peak emission. Calculation results suggest that the shortest intermolecular Cu···Cu distance plays an important role in the emission spectra of the vertical- and tilting-movement dimers, which is ascribed to the variation of the energy gap for the frontier molecular orbitals involved in the main emitting transition. The blue shift of λ_{em} in parallel-movement and rotational dimers can be traced back to the variation of the mutual spatial orientation. Therefore, the modulation of the extent of movement or rotational angles for stacked dimers by external perturbations creates new possibilities for the design of molecular light-emitting devices.

Introduction

Highly luminescent materials, including d^{10} monovalent ions, have been the subjects of increasing attention in the past few years[1−23] because the metal−metal and metal−ligand bonding natures in such materials create the potential for interesting and unique chemical properties. Cyclic trinuclear complexes of d^{10} transition metal ions describe an important class of coordination compounds whose significance spans multiple fundamental areas.[6−17] Omary, Dias, and co-workers have shown that trinuclear complexes of Cu(I) with fluorinated pyrazolate ligands exhibit bright and tunable luminescence that render them attractive candidates for emitting materials in molecular light-emitting device applications, because fluorination facilitates thin-film fabrication and the existence of closed-shell transition metals should enhance the phosphorescence.[13−19] Fluorination also provides other beneficial properties to metal adducts, including improved thermal and oxidative stability and reduced concentration quenching.[16,18−22] The phosphorescence colors and lifetimes of these systems were found to be drastically sensitive to solvent, temperature, concentration, rigidity of medium, substituents on the pyrazolate ring, and identity of the coinage metal.[12d,15−17,19,23]

In recent years, a number of studies have demonstrated that the interplay between theory and experiment is capable of providing useful insights into the understanding of the molecular electronic structure of the ground and excited-state as well as the nature of absorption and photoluminescence.[24−35] A quantitative correlation between the variation of the molecular geometry and the optical properties is of great importance for designing new materials with improved properties for applications such as optoelectronic. Density functional theory (DFT)[36] has been remarkably successful to accurately evaluate a variety of ground state properties of large systems and, in particular, of complexes containing transition metals.[24−32] Time-dependent DFT approach (TD−DFT)[37−39] has become an important tool for the study of excited states properties and, in particular, for the calculation of vertical electronic excitation spectra.[25−35]

The experimental emission spectrum features for trinuclear coinage metal pyrazolates $\{[3,5\text{-}(CF_3)_2Pz]Cu\}_3$ were found that the orange emission at 77 K is due to the combination of two bands (a major red peak at ∼665 nm and a yellow shoulder at ∼590 nm), while the yellow shoulder disappears at higher temperatures, leaving only the red emission.[16] Crystal structures for $\{[3,5\text{-}(CF_3)_2Pz]Cu\}_3$ revealed that there are two stacking modes in the neighboring dimers.[16] To the best of our knowledge, no detail theoretical investigation has been performed for this system to explain the different emission features under different temperatures, although very recently Omary and Dias et al. have performed theoretical investigation to explore the ground and phosphorescent excited states of trinuclear coinage metal pyrazolates in mono trinuclear complex and two

* Corresponding author. Fax: +86-431-85684937. E-mail: zhangjp162@nenu.edu.cn.
[†] Northeast Normal University.
[‡] Jilin Normal University.

10.1021/jp0689215 CCC: $37.00
Published on Web 05/19/2007

TABLE 1: M and D_1 λ_{em} (nm) as Function of Calculation Method and Basis Set

	BPW91	B3PW91	BP86	B3P86	BLYP	B3LYP	SVWN5	exp
				{[3,5-$(CF_3)_2$Pz]Cu}$_3$ (**M**)				
6-31G	598.53	612.58	599.50	607.57	583.65	597.14	579.60	665[a]
6-31G*	608.31	607.90	609.06	602.81	591.92	592.28	589.15	663[b]
LANL2DZ	456.67	414.71	455.55	410.23	446.92	407.90	440.82	
				{[(3,5-$(CF_3)_2$Pz)Cu]$_3$}$_2$ (**D_1**)				
6-31G	634.89	649.35	633.38	642.30	614.85	629.83	610.52	
6-31G*	640.33	639.51	638.57	632.55	618.76	620.26	615.75	
LANL2D Z	486.68	436.16	484.67	431.35	471.40	425.29	470.76	

[a] Experimental data from ref 16a. [b] Experimental data from ref 16b.

TABLE 2: TD-B3PW91/6-31G Calculated Lowest-Lying Triplet Excited States for Monomer and Pristine Dimers[a]

complex	$\Psi_v \rightarrow \Psi_o$	assignment	E (eV)	λ_{em} (nm)	d_{cu-cu} (Å)
M	LUMO → HOMO (0.81)	^{3}MCCT/^{3}LMCT	2.0240	612.58	
D_1	LUMO+1 → HOMO (0.70)	^{3}MCCT/^{3}LMCT	1.9093	649.35	3.813
D_2	LUMO → HOMO-1 (0.67)	^{3}MCCT/^{3}LMCT	2.0201	613.75	3.987

[a] Ψ_o = occupied and Ψ_v = virtual orbitals that define the transition. The value of the CI coefficient for each transition is given in parentheses. E = energy (eV) of the transition. λ_{em} = the maximum emission wavelength (in nm). d_{cu-cu} = the shortest intermolecular Cu···Cu distance (Å).

TABLE 3: Natural Atomic Orbital Populations of the Ground States and the Corresponding Lowest-Lying Triplets Excited States for the Emission of Monomer and Pristine Dimers, As Provided by HF/6-31G and CIS/6-31G, Respectively

		M			**D_1**			**D_2**		
atom	orbital	Q_{S0}	Q_{T1}	ΔQ_{T1-S0}	Q_{S0}	Q_{T1}	ΔQ_{T1-S0}	Q_{S0}	Q_{T1}	ΔQ_{T1-S0}
Cu	4s	0.489	0.803	0.314	0.476	0.776	0.300	0.489	0.673	0.184
	4p	0.011	0.071	0.060	0.012	0.087	0.075	0.014	0.061	0.047
	3d	9.661	9.263	−0.398	9.668	9.259	−0.409	9.661	9.447	−0.214
Cu	4s	0.482	0.826	0.344	0.467	0.794	0.327	0.464	0.927	0.463
	4p	0.011	0.074	0.063	0.012	0.084	0.072	0.012	0.096	0.084
	3d	9.665	9.230	−0.435	9.672	9.250	−0.422	9.675	9.054	−0.621
$\sum\Delta$Cu[a]			−0.063			−0.149			−0.135	
$\sum\Delta$L[a]			0.067			0.153			0.140	

[a] The differences of Cu(I) centers, organic ligands between the lowest-lying triplet excited-state and ground state in the natural atomic orbital populations. The negative value denotes the increases of orbital population in the electronic transition from T_1 to S_0.

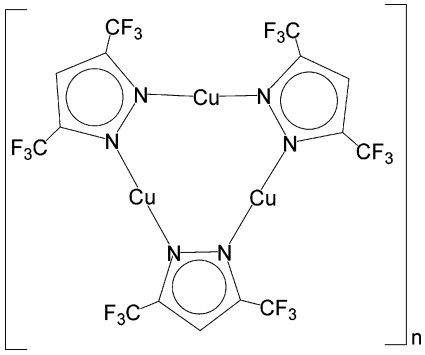

Figure 1. Molecular geometries of {[3,5-$(CF_3)_2$Pz]Cu}$_3$ in the monomeric (n = 1) and dimeric (n = 2) forms. For clarity, hydrogen atoms are not shown.

dimers in special arranged conformations using B3LYP, LMP2, and ROHF methods.[17] In this report, we selected monomer (**M**) and two neighboring stacked dimers (**D**)[16] based on the crystal structure of {[3,5-$(CF_3)_2$Pz]Cu}$_3$ as model complexes to explore the special optical properties of trinuclear copper(I) complexes in depth using various TD−DFT approaches. Furthermore, we investigate that the lowest triplet excited-state (T_1) conformation for stacked dimers affects the emission spectrum. A detailed knowledge of these issues is essential for the understanding of OLED device operation and for the design of novel improved materials.

Computational Methods

Studies of the excited-state properties for a number of molecules using the single configuration interaction (CIS)[40a] method have shown that, despite the tendency of CIS to overestimate electronic transition energies, the excited-state potential energy surface can often be quite accurate, as evidenced by comparison of equilibrium excited-state structure with experiment.[40b−e] The T_1 geometry of the monomer was optimized at the CIS level with the 6-31G[41,42] basis set. The emission spectra of complexes as shown in Figure 1 were investigated by TD−DFT with various functionals, such as the generalized gradient approximations (BLYP,[43,44] BP86,[44,45] BPW91[44,46]), the hybrid functional methods (B3LYP,[43,47,48] B3P86,[45,48−50] B3PW91[48−51]), and the local spin density approach (SVWN5[52,53]). To examine the basis set dependence of the TD−DFT results, we employed the 6-31G, 6-31G*[41,42,54] basis sets, as well as LANL2DZ.[55] Electron population changes associated to the emissive transition ($T_1 \rightarrow S_0$) were investigated through a natural bond orbital (NBO) calculation,[56] using the CIS/6-31G and HF/6-31G methods, respectively. All the calculations were carried out with GAUSSIAN 98[57] suite of programs, except for NBO calculation using GAUSSIAN 03[58] package.

Results and Discussion

Functional and Basis Set Dependence for Investigated System. In order to ascertain the quality of the theoretical

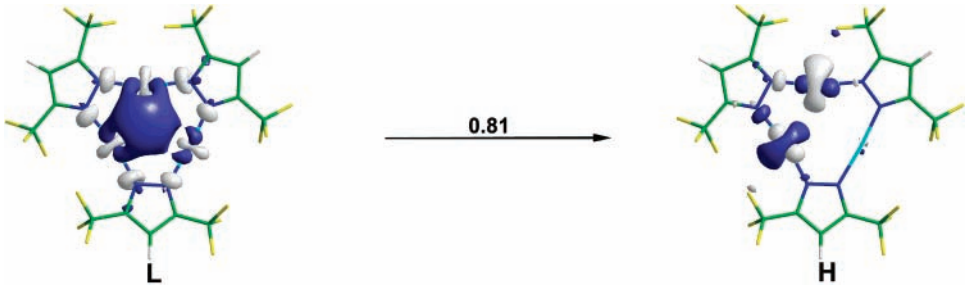

Figure 2. The TD-B3PW91/6-31G calculated triplet electron transition (illustration) for **M**.

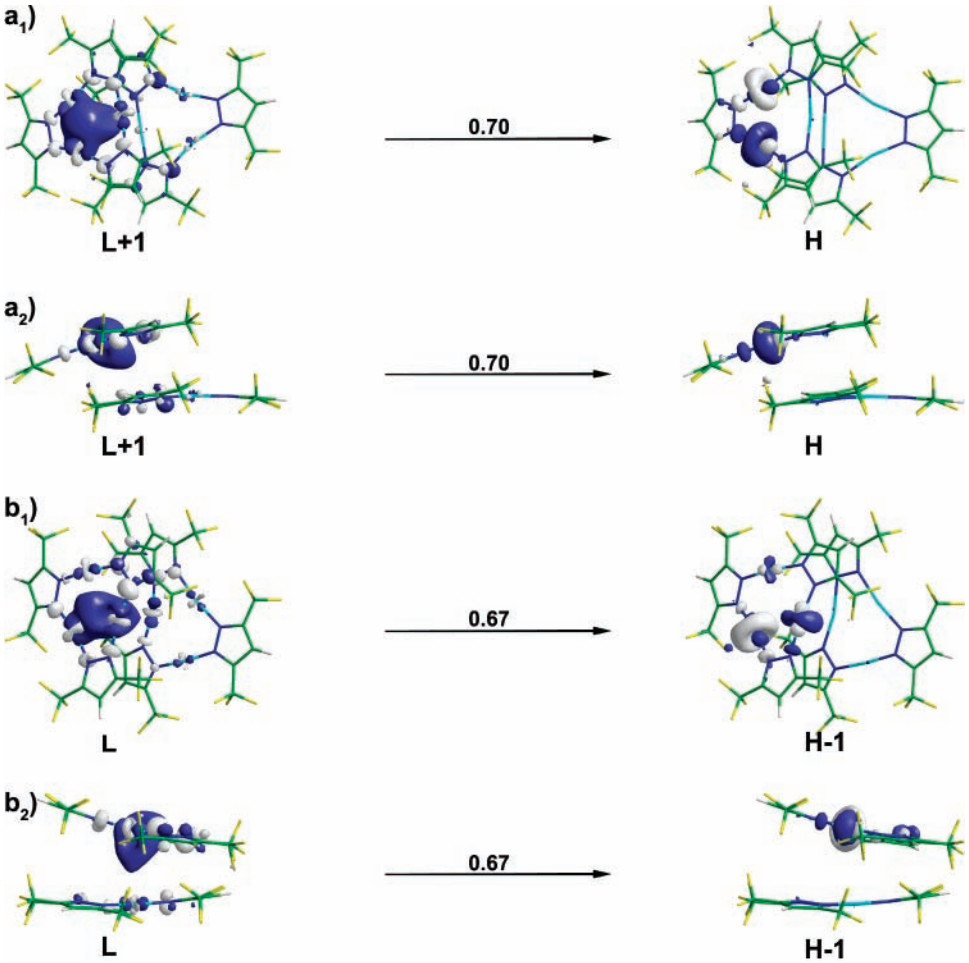

Figure 3. The TD-B3PW91/6-31G calculated triplet electron transitions (illustrations) for $\mathbf{D_1}$ (a_1, top view; a_2, side view) and $\mathbf{D_2}$ (b_1, top view; b_2, side view).

methodology employed, we investigate the functional and basis set dependence of the emission spectrum in detail. The corresponding results are listed in Table 1 as well as the available experimental data for comparison.

From these results, one may find that, for both the monomer and dimer, going from 6-31G to 6-31G*, a slight λ_{em} (the maximum emission wavelength) red shift was predicted by BPW91, BP86, BLYP, and SVWN5 functionals, a slight λ_{em} blue shift being detectable in B3PW91, B3P86 and B3LYP results. With respect to LANL2DZ, the λ_{em} calculated by B3PW91, B3P86, and B3LYP are about 30−50 nm smaller than those in BPW91, BP86, BLYP, and SVWN5 functionals, but all these computed values are not well in accordance with the experimental data,[16] indicating that in the range of the functionals used, LANL2DZ basis set is not appropriate to describe the emission spectrum.

From the results listed in Table 1, we also note that a significant accuracy improvement was achieved (increased by 20−40 nm) in going from monomer to dimer compared with experimental results,[16] which is an indication that the bulk emission spectrum is mainly determined by the dimer rather than the monomer. It is clear that, for the dimer, BPW91, B3PW91, BP86, and B3P86 functionals in conjunction with 6-31G and 6-31G* basis sets are appropriate for the trinuclear Cu(I) pyrazolate complexes to get the relatively reliable predictions on the emission spectra. Since the λ_{em} obtained at the TD-B3PW91/6-31G//CIS/6-31G level is quite close to the experimental value,[16] this chemical model can be reasonably chosen for the rest of the work of the current cases.

Emission Spectra. *1. Monomer.* The results of the TD−DFT calculations for complexes in the corresponding monomeric and dimeric forms are summarized in Table 2. The calculated λ_{em}

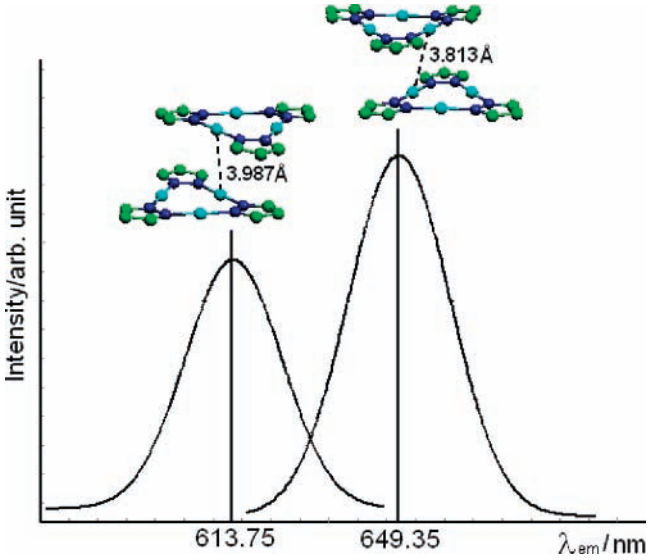

Figure 4. The schematic representation of the emission spectra of complexes **D₂** (left: d_{cu-cu} = 3.987 Å) and **D₁** (right: d_{cu-cu} = 3.813 Å).

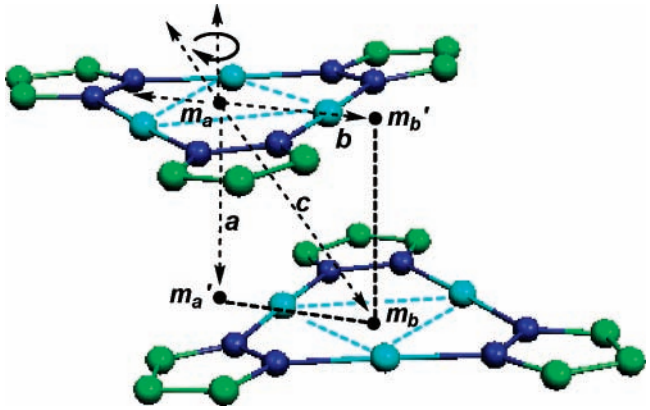

Figure 5. Packing parameters for dimers (substituents and hydrogen atoms are omitted for clarity). m_a and m_b points are the centers of the upper and the lower layers, respectively. m_a' and m_b' points are the vertical projection of the upper m_a and the lower m_b points, respectively. The labels *a*, *b*, and *c* are used to denote the three different movement directions, namely, vertical, parallel, and tilting directions. In the movement plot, the downward arrow represents that the upper layer is moved toward the lower layer along *a*, *b*, and *c* and the upward one represents the upper layer is moved away from the lower layer. In addition, the upper layer is rotated by 60° around the *a* axis.

for **M** is 612.58 nm, which essentially originates from the LUMO → HOMO transition with CI coefficient of 0.81, assigned as the mixture of the metal-centered charge transfer (^{3}MCCT) and ligand-to-metal charge transfer (^{3}LMCT).

To characterize the emission process, we used the difference in the natural atomic orbital populations for the lowest-lying triplet excited-state and the corresponding ground state of Cu(I) centers and organic ligands in **M**. In the emission process, significant charge-transfer localized on two Cu(I) centers. As presented in Table 3, the electronic configurations of two Cu(I) centers with charge transfer in S_0 are $3d^{9.661}4s^{0.489}4p^{0.011}$ and $3d^{9.665}4s^{0.482}4p^{0.011}$, while in T_1, they are $3d^{9.263}4s^{0.803}4p^{0.071}$ and $3d^{9.230}4s^{0.826}4p^{0.074}$, respectively, which indicates that the 4s and 4p electrons transfer back to 3d orbitals during the phosphorescence, and the 4s orbital plays a dominant role. In addition, there is some charge transfer between Cu(I) centers and organic ligands. Therefore, the emission was assigned to ^{3}MCCT mixed with some ^{3}LMCT, which can be well understood by analyzing the single electron transition diagram as shown in Figure 2.

The density diagrams of the frontier molecular orbitals (FMOs) for emitting transitions (Figure 2) can intuitively illustrate the significant electron transitions. In the emission process, the LUMO → HOMO configuration has the largest coefficient (0.81) in the CI wave functions, and is responsible for the emission. As shown in Figure 2, the LUMO concentrates mainly on the s, p orbitals of Cu(I) (Cu-s,p), the remaining contributions being derived from σ orbitals formed by lone pair electrons of nitrogen atoms and d orbitals of Cu(I) (Cu-d), while the HOMO is heavily weighed on the Cu-d. Therefore, the emitting transition is assigned to be $(sp)_\sigma \rightarrow d_{\sigma^*}$ mixed with some ligand-to-metal transition in nature, where $(sp)_\sigma$ denotes a σ-bonding orbital with a mixed s and p orbital character. In addition, the significant overlapping induced by Cu-s,p in the LUMO explains why the Cu(I)···Cu(I) interaction is strongly enhanced in the excited state. In T_1, the shortest Cu···Cu distance of 2.820 Å, close to the estimated sum of the van der Waals radii of two copper atoms (2.800 Å),[59] enables the two Cu(I) s and p orbitals to overlap and form a σ bond, indicating that the cuprophilic interaction is dramatically strengthened.

2. Pristine Dimers. Due to the large size of the dimeric form of the studied complexes, it was difficult/impossible to succeed in the corresponding T_1 structure optimization, owing to the computational limitations. Therefore, on the basis of the crystallographic data,[16] two neighboring S_0 dimers (denoted as pristine dimers) were selected. One (**D₁**) corresponds to the stacked monomers with 3.813 Å of the shortest intermolecular Cu···Cu distance (d_{cu-cu}); the other (**D₂**) corresponds to the neighboring ones with 3.987 Å of d_{cu-cu}, sharing the same monomer with **D₁** in the complex.[16] T_1 structure of the pristine dimer (**D₁** or **D₂**) was constructed by replacing each of the corresponding S_0 monomers in the dimer with its optimized T_1 structure (i.e., as superposition of two T_1 structures of the monomer).

From the calculated results for the emission of **D₁** and **D₂** as listed in Table 2, one may find that the λ_{em} are predicted at 649.35 and 613.75 nm, respectively, the corresponding transitions mainly arising from LUMO+1 → HOMO and LUMO → HOMO-1 transitions, respectively, which are assigned as ^{3}MCCT/^{3}LMCT.

Indeed, by comparing the natural atomic orbital population between the lowest-lying triplet excited states and their corresponding ground states as listed in Table 3, the emission of **D₁** and **D₂** could be attributed to electronic transition within Cu(I) centers, mixed with some ^{3}LMCT transition. For instance, in the case of **D₁**, significant charge transfer within Cu(I) centers are mainly localized on two Cu(I). Their electronic configurations are $3d^{9.668}4s^{0.476}4p^{0.012}$ and $3d^{9.672}4s^{0.467}4p^{0.012}$ in S_0, while in T_1, they are $3d^{9.259}4s^{0.776}4p^{0.087}$ and $3d^{9.250}4s^{0.794}4p^{0.084}$, respectively. This is an indication that the 4s and 4p electrons transfer back to 3d orbitals during the phosphorescence. Additionally, there is some charge transfer between the Cu(I) centers and the organic ligands. The same observation was also found for **D₂**.

Figure 3 shows the FMOs involved in the main emitting transitions for **D₁** and **D₂**, respectively. In the case of **D₁**, the transition is mainly contributed by LUMO+1 → HOMO configuration with CI coefficient of 0.70. As shown in Figure $3a_2$, the electron density in the LUMO+1 and HOMO is almost localized over the same one monomer. The LUMO is composed mainly of the Cu-s,p, the remaining contributions from σ orbitals formed by lone pair electrons of nitrogen atoms and Cu-d, the HOMO being found to largely consist of the Cu-d. Therefore, the emitting transition can be classically described as an

TABLE 4: TD-B3PW91/6-31G Calculated Lowest-Lying Triplet Excited States for Movement Dimers[a]

complex	$\Psi_v \rightarrow \Psi_o$	assignment	E (eV)	λ_{em} (nm)	d_{cu-cu} (Å)
		vertical-movement dimers			
$\mathbf{D_{v1}}$	LUMO → HOMO (0.65)	^{3}MCCT/^{3}LMCT	1.6204	765.14	3.183
$\mathbf{D_{v2}}$	LUMO → HOMO (0.65)	^{3}MCCT/^{3}LMCT	1.6684	743.14	3.239
$\mathbf{D_{v3}}$	LUMO → HOMO (0.66)	^{3}MCCT/^{3}LMCT	1.7887	693.15	3.430
$\mathbf{D_{v4}}$	LUMO+1 → HOMO (0.69)	^{3}MCCT/^{3}LMCT	1.8625	665.68	3.621
$\mathbf{D_1}$	LUMO+1 → HOMO (0.70)	^{3}MCCT/^{3}LMCT	1.9093	649.35	3.813
$\mathbf{D_{v5}}$	LUMO+1 → HOMO (0.71)	^{3}MCCT/^{3}LMCT	1.9393	639.31	4.006
$\mathbf{D_{v6}}$	LUMO+1 → HOMO (0.72)	^{3}MCCT/^{3}LMCT	1.9585	633.05	4.200
$\mathbf{D_{v7}}$	LUMO+1 → HOMO (0.72)	^{3}MCCT/^{3}LMCT	1.9710	629.03	4.394
		parallel-movement dimers			
$\mathbf{D_{p1}}$	LUMO → HOMO (0.52)	^{3}MCCT/^{3}LMCT	1.9254	643.92	4.053
	LUMO → HOMO-1 (0.47)	^{3}MCCT/^{3}LMCT			
	LUMO+1 → HOMO-1 (−0.38)	^{3}MCCT/^{3}LMCT			
$\mathbf{D_{p2}}$	LUMO → HOMO-1 (0.69)	^{3}MCCT/^{3}LMCT	1.9288	642.81	3.930
$\mathbf{D_{p3}}$	LUMO → HOMO-2 (0.64)	^{3}MCCT/^{3}LMCT	1.9426	638.25	3.897
$\mathbf{D_{p4}}$	LUMO → HOMO-1 (0.61)	^{3}MCCT/^{3}LMCT	1.9347	640.82	4.027
	LUMO+1 → HOMO-1 (−0.49)	^{3}MCCT/^{3}LMCT			
$\mathbf{D_1}$	LUMO+1 → HOMO (0.70)	^{3}MCCT/^{3}LMCT	1.9093	649.35	3.813
$\mathbf{D_{p5}}$	LUMO+1 → HOMO (0.59)	^{3}MCCT/^{3}LMCT	1.9154	647.29	3.736
	LUMO+2 → HOMO (0.49)	^{3}MCCT/^{3}LMCT			
$\mathbf{D_{p6}}$	LUMO+2 → HOMO (−0.53)	^{3}MCCT/^{3}LMCT	1.9453	637.33	3.701
	LUMO+1 → HOMO (0.52)	^{3}MCCT/^{3}LMCT			
		rotational dimers			
$\mathbf{D_1}$	LUMO+1 → HOMO (0.70)	^{3}MCCT/^{3}LMCT	1.9093	649.35	3.813
$\mathbf{D_{60}}$	LUMO+1 → HOMO (0.78)	^{3}MCCT/^{3}LMCT	1.9864	624.17	3.876
$\mathbf{D_{120}}$	LUMO → HOMO-1 (0.64)	^{3}MCCT/^{3}LMCT	1.9805	626.01	3.747
	LUMO+2 → HOMO-1 (0.47)	^{3}MCCT/^{3}LMCT			
$\mathbf{D_{180}}$	LUMO+1 → HOMO (0.75)	^{3}MCCT/^{3}LMCT	2.1043	589.19	3.829
$\mathbf{D_{240}}$	LUMO+1 → HOMO (−0.57)	^{3}MCCT/^{3}LMCT	1.9774	627.01	3.774
	LUMO → HOMO (0.51)	^{3}MCCT/^{3}LMCT			
$\mathbf{D_{300}}$	LUMO+1 → HOMO-1 (0.57)	^{3}MCCT/^{3}LMCT	1.9957	621.26	3.920
	LUMO+1 → HOMO (-0.53)	^{3}MCCT/^{3}LMCT			
		tilting-movement dimers			
$\mathbf{D_{t1}}$	LUMO → HOMO (−0.64)	^{3}MCCT/^{3}LMCT	1.7756	698.26	3.427
$\mathbf{D_{t2}}$	LUMO+1 → HOMO (0.52)	^{3}MCCT/^{3}LMCT	1.8068	686.19	3.490
	LUMO → HOMO (0.50)	^{3}MCCT/^{3}LMCT			
$\mathbf{D_{t3}}$	LUMO+1 → HOMO (0.63)	^{3}MCCT/^{3}LMCT	1.8477	671.03	3.590
$\mathbf{D_{t4}}$	LUMO+1 → HOMO (0.67)	^{3}MCCT/^{3}LMCT	1.8804	659.36	3.698
$\mathbf{D_1}$	LUMO+1 → HOMO (0.70)	^{3}MCCT/^{3}LMCT	1.9093	649.35	3.813
$\mathbf{D_{t5}}$	LUMO+1 → HOMO (0.72)	^{3}MCCT/^{3}LMCT	1.9339	641.12	3.936
$\mathbf{D_{t6}}$	LUMO+1 → HOMO (0.73)	^{3}MCCT/^{3}LMCT	1.9526	634.96	4.064
$\mathbf{D_{t7}}$	LUMO+1 → HOMO (0.74)	^{3}MCCT/^{3}LMCT	1.9679	630.02	4.198

[a] Ψo = occupied and Ψv = virtual orbitals that define the transition. The value of the CI coefficient for each transition is given in parentheses. E = energy (eV) of the transition. λ_{em} = the maximum emission wavelength (in nm). d_{cu-cu} = the shortest intermocular Cu···Cu distance (Å). On the basis of the geometry of $\mathbf{D_1}$, in $\mathbf{D_{n4}} \rightarrow \mathbf{D_{n3}} \rightarrow \mathbf{D_{n2}} \rightarrow \mathbf{D_{n1}}$ (n = v/p/t), the upper layer is gradually moved toward the lower layer along *a*, *b*, and *c* (see in Figure 5), whereas in $\mathbf{D_{n5}} \rightarrow \mathbf{D_{n6}} \rightarrow \mathbf{D_{n7}}$ (n = v/p/t), the upper layer is gradually moved away from the lower layer.

intramolecular metal-centered charge-transfer transition interfered with some ligand-to-metal transition in nature. In addition, we find the shortest intramolecular Cu···Cu distance of 2.820 Å is much shorter than d_{cu-cu} of 3.813 Å in $\mathbf{D_1}$, which is indicative of the existence of the intramolecular cuprophilic interaction, as is also reflected by the significant overlapping induced by Cu-s,p localized on the same monomer in the LUMO. Similar observation has also been observed for $\mathbf{D_2}$.

Systematic experimental studies[16] suggest bright phosphorescent emission of this complex is sensitive to the temperature. The orange emission at 77 K is due to the combination of two bands, a major red peak at ~665 nm and a yellow shoulder at ~590 nm.[16] The yellow shoulder disappears at higher temperatures, leaving only the red emission, but band broadening at room temperature leads to orange emission.[16] From the calculated results listed in Table 2, one can find that the predicted λ_{em} are close to experimental values[16] of ~665 and ~590 nm, respectively, for $\mathbf{D_1}$ (649.35 nm) and $\mathbf{D_2}$ (613.75 nm), indicating that the phosphorescence bands can be assigned to neighboring stacked dimers with shorter and longer d_{cu-cu} in the complex, respectively (as shown in Figure 4). Energy transfer from T_1 of $\mathbf{D_2}$ to that of $\mathbf{D_1}$ through the shared monomer for stacked dimers is responsible for the disappearance of the shoulder, leaving only the main peak of $\mathbf{D_1}$ upon heating.[16]

Systematic experimental studies[16] also suggest that the direct impact of slight compressions of metal···metal distances (e.g., d_{cu-cu} for $\{[3,5\text{-}(CF_3)_2Pz]Cu\}_3$ at RT and 100 K are 3.879 and 3.813 Å) is usually a gradual red shift in λ_{em} upon cooling. Therefore, in the following sections, we further investigate the T_1 conformational dependence of the dimer $\mathbf{D_1}$ (λ_{em} corresponds to the main peak) for the emission spectra at the same theory level, with the aim to provide insight into the nature of optical characteristics.

3. T_1 Conformations Dependence for Emission Spectra. A schematic representation of all T_1 conformations selected is shown in Figure 5. We ran a batch of simulations to explore the relationship between T_1 conformations and the optical properties by varying the extent of movement or rotational angles based on the T_1 geometry of $\mathbf{D_1}$, that is, the T_1 geometry of $\mathbf{D_1}$ as the starting geometry, one molecule (the lower layer) is fixed, whereas the other one (the upper layer) is linearly shifted along *a*, *b*, and *c* directions, or rotated by 60° around *a*

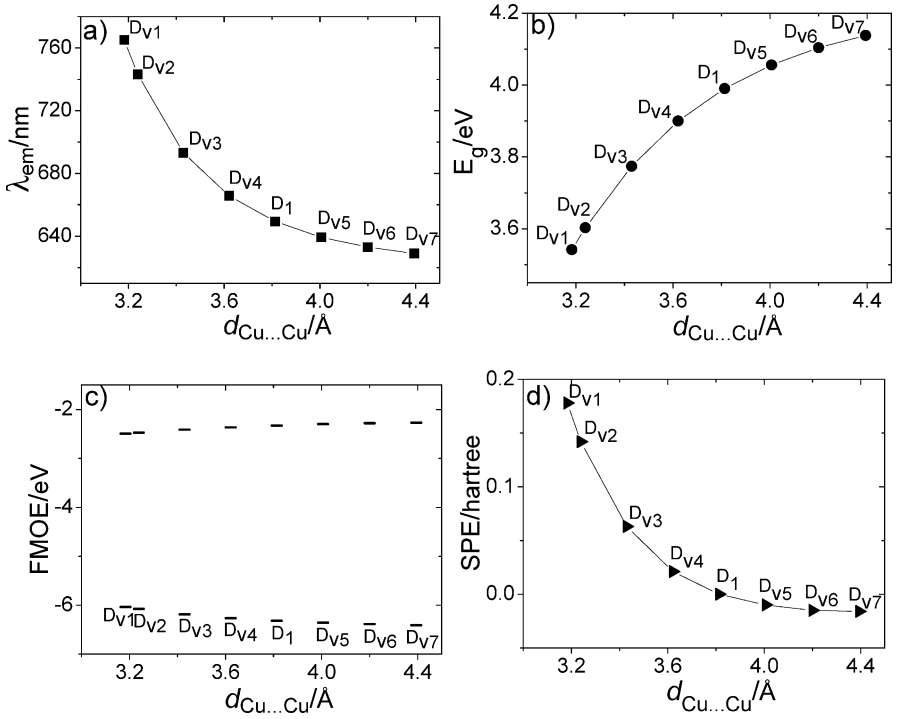

Figure 6. Plots of (a) λ_{em}, (b) E_g, (c) FMOE, and (d) SPE vs d_{cu-cu}.

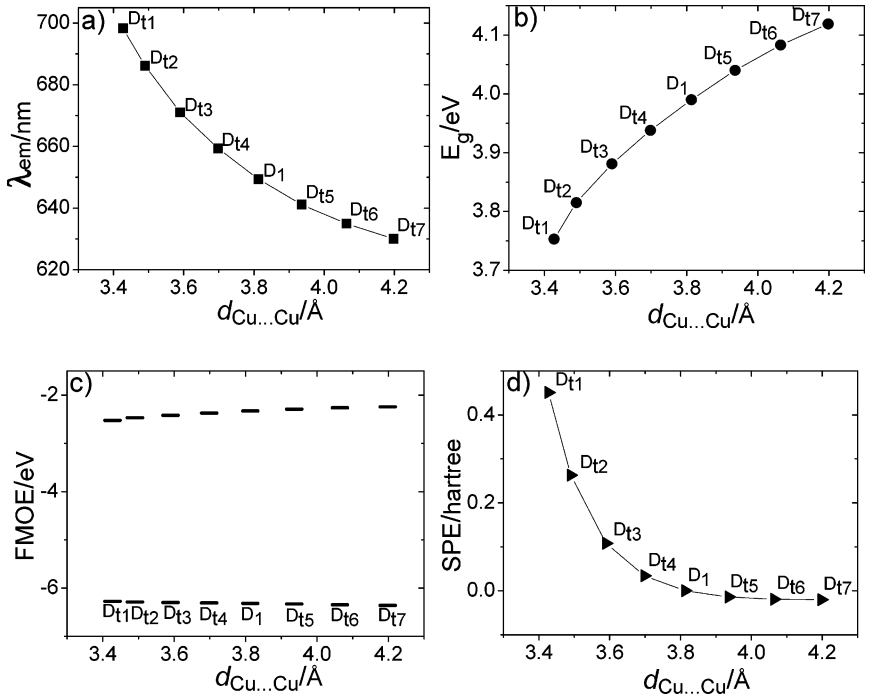

Figure 7. Plots of (a) λ_{em}, (b) E_g, (c) FMOE, and (d) SPE vs d_{cu-cu}.

axis, respectively. The results of the TD−DFT calculations for various T_1 conformations are listed in Table 4.

3.1. λ_{em} Shifts upon Various T_1 Conformations. From the calculated results in Table 4, one may figure out that from $\mathbf{D_{v7}}$ to $\mathbf{D_1}$ and then to $\mathbf{D_{v1}}$, the λ_{em} red shifts from 629.03 to 765.14 nm, is accompanied by a dramatic decrease in d_{cu-cu} (4.394−3.183 Å). It should be noted that considerable changes in d_{cu-cu} can result in rather large changes in λ_{em}, indicating that the emission spectrum is strongly related to d_{cu-cu}.

Figure 6 illustrates the good relationship between the optical properties (e.g., λ_{em}, the energy gap for FMOs (E_g) involved in the main emitting transition, the energy for FMOs (FMOE) involved in the main emitting transition, single point energy (SPE)) and d_{cu-cu} for vertical-movement dimers, and the corresponding data in detailed are collected in Supporting Information (Table S1). As can be seen from Figure 6a, the shorter d_{cu-cu} is, the more obvious the red shift in λ_{em} are. This trend agrees well with the experimental observation.[16] The change for λ_{em} can be simply traced back to the variation of E_g because the main emitting transition generally dominates the emission process. Figure 6b shows that E_g decays with the decrease of d_{cu-cu}. E_g can be quantitatively correlated with

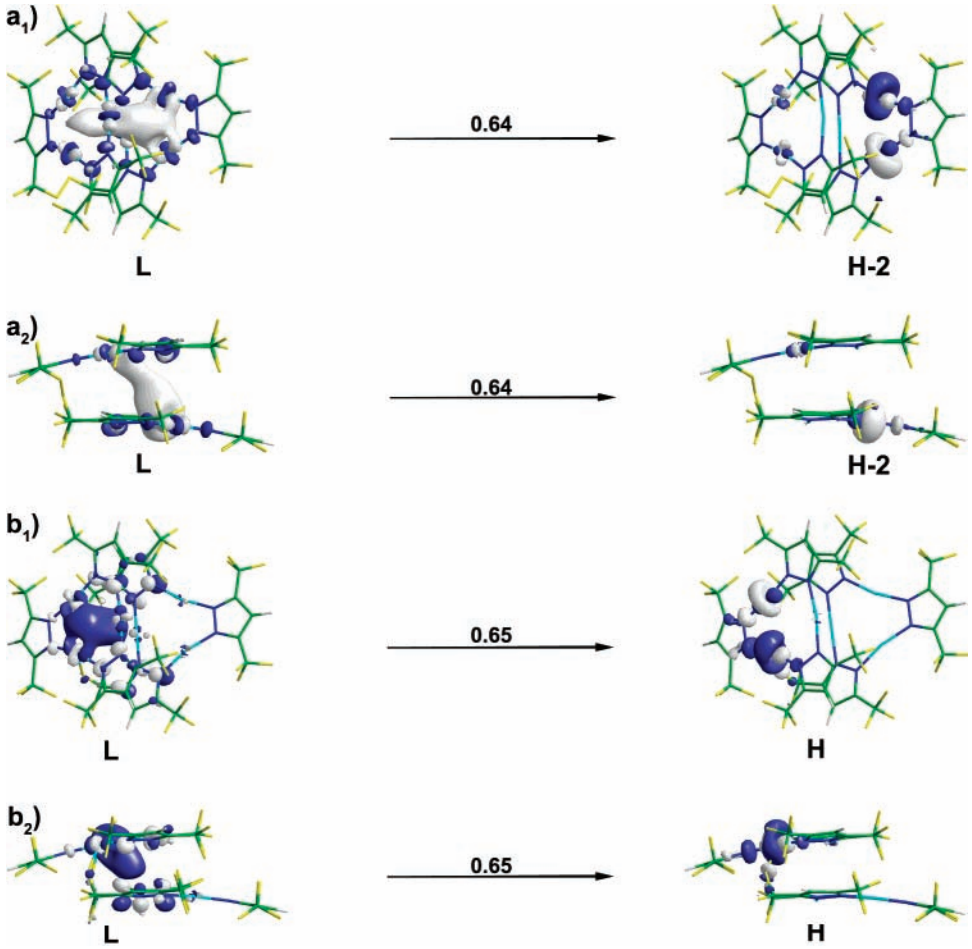

Figure 8. The TD-B3PW91/6-31G calculated triplet electron transition (illustrations) for $\mathbf{D_{p3}}$ (a_1, top view; a_2, side view) and $\mathbf{D_{v1}}$ (b_1, top view; b_2, side view).

FMOE. The evolution of FMOE as functions of d_{cu-cu} is depicted in Figure 6c. The decrease of d_{cu-cu} raises the HOMO level and lowers the LUMO level, the net effect being the E_g decreasing. Therefore, the λ_{em} is dependent on d_{cu-cu} by the variation of E_g. Further quantitative analyses show that SPE varies with d_{cu-cu}, as depicted in Figure 6d. Here, SPE of $\mathbf{D_1}$ is referred to as zero. From $\mathbf{D_{v7}}$ to $\mathbf{D_1}$ and then to $\mathbf{D_{v1}}$, the SPE are increasing gradually with the decreases of d_{cu-cu}, which indicates that the intermolecular repulsion increases.

Unlike the vertical-movement dimers, in comparison with that of $\mathbf{D_1}$, a slight λ_{em} blue shift was predicted for parallel movement ($\mathbf{D_{p1}}-\mathbf{D_{p6}}$), in the range from 637.33 to 647.29 nm. Moreover, the corresponding d_{cu-cu} does not change considerably (4.053−3.701 Å). This can be explained by the variation of the mutual spatial orientation between two molecules. d_{cu-cu} may not be the crucial factor to affect the emission spectra. Similar trend has been also found in all rotational dimers. Indeed, the λ_{em} predicted for all the rotational dimers are strongly blue-shifted with respect to $\mathbf{D_1}$, especially for $\mathbf{D_{180}}$ (589.19 nm), whereas all the corresponding d_{cu-cu} slightly change (3.920−3.747 Å). This can be explained in the same way by the variation of the mutual spatial orientation by the rotation rather than d_{cu-cu}.

In the tilting case, we attempt to consider the combined effects of the vertical and parallel movements on the emission spectrum. As expected, the net effect is that λ_{em} shift toward the red (from 630.02 to 698.26 nm) and simultaneously a decrease of d_{cu-cu} is observed (4.198−3.427 Å) going from $\mathbf{D_{t7}}$ to $\mathbf{D_1}$ and then to $\mathbf{D_{t1}}$. The trend which is similar to that of vertical-movement dimers allows us to deduce that the effect of parallel movement on the emission spectrum cannot compete with that of vertical movement. Therefore the linear decrease of d_{cu-cu} is responsible for the λ_{em} red shift. Figure 7 shows the dependence of the optical properties (e.g., λ_{em}, E_g, FMOE, SPE) on d_{cu-cu} for tilting-movement dimers, the corresponding data are given in Supporting Information (Table S1). Obviously, the dependence of λ_{em}, E_g, FMOE, and SPE on d_{cu-cu} in tilting-movement dimers is similar to that of vertical-movement dimers (see Figures 6 and 7). Therefore, the dependency of λ_{em} on d_{cu-cu} can be ascribed to the variation of E_g.

Finally, from the calculated results listed in Table 4, one may find that the predicted λ_{em} of $\mathbf{D_{v4}}$ (665.68 nm) agrees well with experimental one (665/663 nm),[16] indicating that d_{cu-cu} may be reduced in T_1, comparatively to that in the corresponding ground state.

3.2. Emissive Transition Character Analysis. Table S2 (in Supporting Information) contains the natural atomic orbital populations of the lowest-lying triplet excited states and their corresponding ground states for all investigated dimers. All dimers in various conformations possess a pronounced charge-transfer character, where the electron transfers from the 4s and 4p orbitals of Cu(I) back to 3d orbital during the phosphorescence. Additionally, there is some charge transfer between the Cu(I) centers and the organic ligands. Therefore, all the emitting transitions were assigned to ^{3}MCCT/^{3}LMCT.

Indeed, for all the dimers in various conformations, the dominant transition has the same mixed character as ^{3}MCCT/^{3}LMCT. As shown in Supporting Information (Figures S1−S4), the virtual orbital largely consists of Cu-s,p, the remaining

contributions arising from σ orbitals formed by lone pair electrons of nitrogen atoms and Cu-d, whereas the occupied one is essentially composed of the Cu-d. Therefore, the emitting transition is also assigned to be $(sp)_{\sigma} \rightarrow d_{\sigma^*}$ perturbed by some ^{3}LMCT transition.

It is worthwhile to note that a significant difference can be observed in the virtual orbitals involved in the main emitting transitions of parallel-movement dimers comparatively to those in the case of vertical-, tilting-movement, and rotational dimers. Indeed, when the upper molecule is gradually moved to the core of the lower one in the parallel-movement dimers, the intermolecular orbital overlapping resulted from the same phase of the orbitals increases (e.g., $\mathbf{D_{p3}}$, see Figure 8(a_1/a_2)). This indicates the existence of the intermolecular Cu···Cu interaction though d_{cu-cu} is more than 3.701 Å, which is much longer than the estimated sum of the van der Waals radii of two copper atoms (2.800 Å).[59] However, the intermolecular Cu···Cu interaction should not be the crucial factor to affect the emission spectra because a slight λ_{em} blue shift was predicted comparatively to that of $\mathbf{D_1}$. For the rest of the dimers, even though d_{cu-cu} greatly shortens from 4.394 Å ($\mathbf{D_{v7}}$) to 3.183 Å ($\mathbf{D_{v1}}$), still longer than the shortest intramolecular one of 2.820 Å, a significant intramolecular overlapping induced by Cu-s,p exists in the virtual orbital involved in the main emitting transitions, indicating the presence of the intramolecular cuprophilic interaction between Cu(I) centers (see Figure 8 (b_1/b_2)).

Finally, in order to verify the computational results in our work, we have carried out the same calculations on all the complexes using B3P86 and B3LYP functionals, similar trends of the emission spectra have been found (see Tables S3−S5 in Supporting Information). Therefore, we believe that the present study is reliable for interpreting the experimental emission spectra features and for understanding the effects of the T_1 conformation on the emission spectra.

Conclusions

In this paper, we have used theoretical approaches based on DFT to examine the optical properties of $\{[3,5\text{-}(CF_3)_2Pz]Cu\}_3$ in monomeric and dimeric forms. The emission of all complexes originates from T_1, and the corresponding emissive states are assigned as ^{3}MCCT/^{3}LMCT. The emission spectrum features are interpreted in detail. The bulk emission spectrum of this complex is mainly determined by the dimer rather than the monomer. The predicted λ_{em} are close to experimental values of ~665 and ~590 nm respectively for neighboring stacked dimers with shorter ($\mathbf{D_1}$, 649.35 nm) and longer ($\mathbf{D_2}$, 613.75 nm) d_{cu-cu}, while the neighboring stacked dimers share the same monomer. Energy transfer from T_1 of $\mathbf{D_2}$ to that of $\mathbf{D_1}$ through the shared monomer is responsible for the disappearance of the shoulder, leaving only the main peak upon heating.

In order to probe the effect of the T_1 conformation on the emission spectra, the optical properties of various dimers were investigated by varying the extent of movement or rotational angles based on the T_1 geometry of $\mathbf{D_1}$ for the first time. It was found that, d_{cu-cu} played an important role in the emission spectra of the vertical- and tilting-movement dimers. Actually, the λ_{em} is dependent on d_{cu-cu} by the variation of E_g. The blue shift of λ_{em} in parallel-movement and rotational dimers can be attributed to the variation of the mutual spatial orientation. The modulation of the extent of movement or rotational angles by external perturbations creates new possibilities for the design of molecular light-emitting devices.

Acknowledgment. Financial support from the NSFC (No. 50473032) and NCET-06-0321 is gratefully acknowledged.

Supporting Information Available: Details of the computational results and tables not given in the main text are provided. This material is available free of charge via the Internet at http://pubs.acs.org.

References and Notes

(1) Harvey, P. D.; Drouin, M.; Zhang, T. *Inorg. Chem.* **1997**, *36*, 4998.
(2) Miller, M. T.; Gantzel, P. K.; Karpishin, T. B. *J. Am. Chem. Soc.* **1999**, *121*, 4292.
(3) Felder, D.; Nierengarten, J.-F.; Barigelletti, F.; Ventura, B.; Armaroli, N. *J. Am. Chem. Soc.* **2001**, *123*, 6291.
(4) Yam, V. W.-W.; Yu, K.-L.; Wong, K. M.-C.; Cheung, K.-K. *Organometallics* **2001**, *20*, 721.
(5) Xie, H.; Kinoshita, I.; Karasawa, T.; Kimura, K.; Nishioka, T.; Akai, I.; Kanemoto, K. *J. Phys. Chem. B* **2005**, *109*, 9339.
(6) Vickery, J. C.; Olmstead, M. M.; Fung, E. Y.; Balch, A. L. *Angew. Chem., Int. Ed. Engl.* **1997**, *36*, 1179.
(7) (a) Tsunoda, M.; Gabbaï, F. P. *J. Am. Chem. Soc.* **2000**, *122*, 8335. (b) Burini, A.; Bravi, R.; Fackler, J. P., Jr.; Galassi, R.; Grant, T. A.; Omary, M. A.; Pietroni, B. R.; Staples, R. J. *Inorg. Chem.* **2000**, *39*, 3158. (c) Burini, A.; Fackler, J. P., Jr.; Galassi, R.; Grant, T. A.; Omary, M. A.; Rawashdeh-Omary, M. A.; Peitroni, B. R.; Staples, R. J. *J. Am. Chem. Soc.* **2000**, *122*, 11264.
(8) (a) Olmstead, M. M.; Jiang, F.; Attar, S.; Balch, A. L. *J. Am. Chem. Soc.* **2001**, *123*, 3260. (b) Enomoto, M.; Kishimura, A.; Aida, T. *J. Am. Chem. Soc.* **2001**, *123*, 5608. (c) Rawashdeh-Omary, M. A.; Omary, M. A.; Fackler, J. P., Jr.; Galassi, R.; Pietroni, B. R.; Burini, A. *J. Am. Chem. Soc.* **2001**, *123*, 9689.
(9) (a) Burini, A.; Fackler, J. P., Jr.; Galassi, R.; Macchioni, A.; Omary, M. A.; Rawashdeh-Omary, M. A.; Pietroni, B. R.; Sabatini, S.; Zuccaccia, C. *J. Am. Chem. Soc.* **2002**, *124*, 4570. (b) Hayashi, A.; Olmstead, M. M.; Attar, S.; Balch, A. L. *J. Am. Chem. Soc.* **2002**, *124*, 5791.
(10) (a) Burini, A.; Mohamed, A. A.; Fackler, J. P., Jr. *Comments Inorg. Chem.* **2003**, *24*, 253. (b) Tsipis, A. C.; Tsipis, C. A. *J. Am. Chem. Soc.* **2003**, *125*, 1136. (c) Yang, G.; Raptis, R. G. *Inorg. Chem.* **2003**, *42*, 261.
(11) Tsipis, C. A.; Karagiannis, E. E.; Kladou, P. F.; Tsipis, A. C. *J. Am. Chem. Soc.* **2004**, *126*, 12916.
(12) (a) Omary, M. A.; Mohamed, A. A.; Rawashdeh-Omary, M. A.; Fackler, J. P., Jr. *Coord. Chem. Rev.* **2005**, *249*, 1372. (b) Kishimura, A.; Yamashita, T.; Aida, T. *J. Am. Chem. Soc.* **2005**, *127*, 179. (c) Mohamed, A. A.; Burini, A.; Fackler, J. P., Jr. *J. Am. Chem. Soc.* **2005**, *127*, 5012. (d) Omary, M. A.; Rawashdeh-Omary, M. A.; Gonser, M. W. A.; Elbjeirami, O.; Grimes, T.; Cundari, T. R.; Diyabalanage, H. V. K.; Palehepitiya Gamage, C. S.; Dias, H. V. R. *Inorg. Chem.* **2005**, *44*, 8200. (e) Burress, C.; Elbjeirami, O.; Omary, M. A.; Gabbaï, F. P. *J. Am. Chem. Soc.* **2005**, *127*, 12166.
(13) Haneline, M. R.; Tsunoda, M.; Gabbaï, F. P. *J. Am. Chem. Soc.* **2002**, *124*, 3737.
(14) Omary, M. A.; Kassab, R. M.; Haneline, M. R.; Elbjeirami, O.; Gabbaï, F. P. *Inorg. Chem.* **2003**, *42*, 2176.
(15) Dias, H. V. R.; Diyabalanage, H. V. K. *Polyhedron* **2006**, *25*, 1655.
(16) (a) Dias, H. V. R.; Diyabalanage, H. V. K.; Rawashdeh-Omary, M. A.; Franzman, M. A.; Omary, M. A. *J. Am. Chem. Soc.* **2003**, *125*, 12072. (b) Dias, H. V. R.; Diyabalanage, H. V. K.; Eldabaja, M. G.; Elbjeirami, O.; Rawashdeh-Omary, M. A.; Omary, M. A. *J. Am. Chem. Soc.* **2005**, *127*, 7489.
(17) Grimes, T.; Omary, M. A.; Dias, H. V. R.; Cundari, T. R. *J. Phys. Chem. A* **2006**, *110*, 5823.
(18) (a) Adachi, C.; Baldo, M. A.; Forrest, S. R. *J. Appl. Phys.* **2000**, *87*, 8049. (b) Zhang, J.; Kan, S.; Ma, Y.; Shen, J.; Chan, W.; Che, C. *Synth. Met.* **2001**, *121*, 1723. (c) Grushin, V. V.; Herron, N.; LeCloux, D. D.; Marshall, W. J.; Petrov, V. A.; Wang, Y. *Chem. Commun.* **2001**, *16*, 1494.
(19) Omary, M. A.; Rawashdeh-Omary, M. A.; Diyabalanage, H. V. K.; Dias, H. V. R. *Inorg. Chem.* **2003**, *42*, 8612.
(20) (a) Dias, H. V. R.; Lu, H.-L. *Inorg. Chem.* **1995**, *34*, 5380. (b) Dias, H. V. R.; Kim, H.-J.; Lu, H.-L.; Rajeshwar, K.; de Tacconi, N. R.; Derecskei-Kovacs, A.; Marynick, D. S. *Organometallics* **1996**, *15*, 2994.
(21) (a) Dias, H. V. R.; Jin, W. *J. Am. Chem. Soc.* **1995**, *117*, 11381. (b) Dias, H. V. R.; Jin, W. *Inorg. Chem.* **1996**, *35*, 3687.
(22) Dias, H. V. R.; Lu, H.-L.; Kim, H. J.; Polach, S. A.; Goh, T. K. H. H.; Browning, R. G.; Lovely, C. J. *Organometallics* **2002**, *21*, 1466.
(23) Dias, H. V. R.; Polach, S. A.; Wang, Z. *J. Fluorine Chem.* **2000**, *103*, 163.
(24) (a) Guckian, A. L.; Doering, M.; Ciesielski, M.; Walter, O.; Hjelm, J.; O'Boyle, N. M.; Henry, W.; Browne, W. R.; McGarvey, J. J.; Vos, J. G. *Dalton Trans.* **2004**, 3943. (b) Zhang, J.; Wang, R. *Synth. Met.* **2005**, *152*, 241. (c) D'Souza, F.; Smith, P. M.; Rogers, L.; Zandler, M. E.; Islam, D. M. S.; Araki, Y.; Ito, O. *Inorg. Chem.* **2006**, *45*, 5057. (d) O'Boyle, N. M.; Albrecht, T.; Murgida, D. H.; Cassidy, L.; Ulstrup, J.; Vos, J. G. *Inorg. Chem.* **2007**, *46*, 117. (e) Gahungu, G.; Zhang, B.; Zhang, J. *J. Phys. Chem. B* **2006**, *110*, 16852.

(25) (a) Abedin-Siddique, Z.; Ohno, T.; Nozaki, K. *Inorg. Chem.* **2004**, *43*, 663. (b) Fantacci, S.; De Angelis, F.; Wang, J.; Bernhard, S.; Selloni, A. *J. Am. Chem. Soc.* **2004**, *126*, 9715. (c) Zhang, J.; Frenking, G. *J. Phys. Chem. A* **2004**, *108*, 10296. (d) Browne, W. R.; O'Boyle, N. M.; Henry, W.; Guckian, A. L.; Horn, S.; Fett, T.; O'Connor, C. M.; Duati, M.; De Cola, L.; Coates, C. G.; Ronayne, K. L.; McGarvey, J. J.; Vos, J. G. *J. Am. Chem. Soc.* **2005**, *127*, 1229. (e) Browne, W. R.; O'Boyle, N. M.; McGarvye, J. J.; Vos, J. G. *Chem. Soc. Rev.* **2005**, *34*, 641. (f) Gahungu, G.; Zhang, J. *J. Phys. Chem. B* **2005**, *109*, 17762. (g) Gahungu, G.; Zhang, J. *THEOCHEM* **2005**, *755*, 19.

(26) (a) Zhang, J.; Frenking, G. *Chem. Phys. Lett.* **2004**, *394*, 120. (b) Rosa, A.; Ricciardi, G.; Baerends, E. J.; Zimin, M.; Rodgers, M. A. J.; Matsumoto, S.; Ono, N. *Inorg. Chem.* **2005**, *44*, 6609. (c) Nazeeruddin, M. K.; Angelis, F. D.; Fantacci, S.; Selloni, A.; Viscardi, G.; Liska, P.; Ito, S.; Takeru, B.; Grätzel, M. *J. Am. Chem. Soc.* **2005**, *127*, 16835. (d) Horsman, G. P.; Jirasek, A.; Vaillancourt, F. H.; Barbosa, C. J.; Jarzecki, A. A.; Xu, C.; Mekmouche, Y.; Spiro, T. G.; Lipscomb, J. D.; Blades, M. W.; Turner, R. F. B.; Eltis, L. D. *J. Am. Chem. Soc.* **2005**, *127*, 16882. (e) Mack, J.; Asano, Y.; Kobayashi, N.; Stillman, M. J. *J. Am. Chem. Soc.* **2005**, *127*, 17697. (f) Barolo, C.; Nazeeruddin, M. K.; Fantacci, S.; Censo, D. D.; Comte, P.; Liska, P.; Viscardi, G.; Quagliotto, P.; Angelis, F. D.; Ito, S.; Grätzel, M. *Inorg. Chem.* **2006**, *45*, 4642. (g) Lam, W. H.; Cheng, C.; Yam, V. W. *Inorg. Chem.* **2006**, *45*, 9434.

(27) (a) Petit, L.; Maldivi, P.; Adamo, C. *J. Chem. Theory Comput.* **2005**, *1*, 953. (b) Jorge, F. E.; Autschbach, J.; Ziegler, T. *J. Am. Chem. Soc.* **2005**, *127*, 975. (c) Gahungu, G.; Zhang, J. *Chem. Phys. Lett.* **2005**, *410*, 302. (d) Lundqvist, M. J.; Nilsing, M.; Lunell, S.; Akermark, B.; Persson, P. *J. Phys. Chem. B* **2006**, *110*, 20513. (e) Ghosh, S.; Chaitanya, G. K.; Bhanuprakash, K.; Nazeeruddin, M. K.; Grätzel, M.; Reddy, Y. P. *Inorg. Chem.* **2006**, *45*, 7600. (f) Fernádez, E. J.; Laguna, A.; Lépez-de-Luzuriaga, J. M.; Monge, M.; Montiel, M.; Olmos, M. E.; Rodríguez-Castillo, M. *Organometallics* **2006**, *25*, 3639. (g) De Angelis, F.; Fantacci, S.; Sgamellotti, A.; Cariati, E.; Ugo, R.; Ford, P. C. *Inorg. Chem.* **2006**, *45*, 10576.

(28) Ciofini, I.; Lainé, P. P.; Bedioui, F.; Adamo, C. *J. Am. Chem. Soc.* **2004**, *126*, 10763.

(29) Boulet, P.; Chermette, H.; Daul, C.; Gilardoni, F.; Rogemond, F.; Weber, J.; Zuber, G. *J. Phys. Chem. A* **2001**, *105*, 885.

(30) Boulet, P.; Chermette, H.; Weber, J. *Inorg. Chem.* **2001**, *40*, 7032.

(31) Adamo, C.; Barone, V. *Theor. Chem. Acc.* **2000**, *105*, 169.

(32) Farrell, I. R.; van Slageren, J.; Záliš, S.; Vlček, A., Jr. *Inorg. Chim. Acta* **2001**, *315*, 44.

(33) (a) Jödicke, C. J.; Lüthi, H. P. *J. Am. Chem. Soc.* **2003**, *125*, 252. (b) Belletête, M.; Morin, J. F.; Leclerc, M.; Durocher, G. *J. Phys. Chem. A* **2005**, *109*, 6953. (c) Fabiano, E.; Sala, F. D.; Barbarella, G.; Lattante, S.; Anni, M.; Sotgiu, G.; Hättig, C.; Cingolani, R.; Gigli, G. *J. Phys. Chem. B* **2006**, *110*, 18651. (d) Oliva, M. M.; Casado, J.; Hennrich, G.; López Navarrete, J. T. *J. Phys. Chem. B* **2006**, *110*, 19198.

(34) (a) Lukeš, V.; Aquino, A.; Lischka, H. *J. Phys. Chem. A* **2005**, *109*, 10232. (b) Geskin, V. M.; Grozema, F. C.; Siebbeles, L. D. A.; Beijonne, D.; Brédas, J. L.; Cornil, J. *J. Phys. Chem. B* **2005**, *109*, 20237.

(35) (a) Yang, G.; Liao, Y.; Su, Z.; Zhang, H.; Wang, Y. *J. Phys. Chem. A* **2006**, *110*, 8758. (b) Liang, W. Z.; Zhao, Y.; Sun, J.; Song, J.; Hu, S.; Yang, J. *J. Phys. Chem. B* **2006**, *110*, 9908. (c) Li, Z.; Zhang, J. *Chem. Phys.* **2006**, *331*, 159.

(36) Parr, R. G.; Yang, W. *Density Functional Theory of Atoms and Molecules*; Oxford University Press: Oxford, 1989.

(37) Stratmann, R. E.; Scuseria, G. E.; Frisch, M. J. *J. Chem. Phys.* **1998**, *109*, 8218.

(38) Bauernschmitt, R.; Ahlrichs, R. *Chem. Phys. Lett.* **1996**, *256*, 454.

(39) Casida, M. E.; Jamorski, C.; Casida, K. C.; Salahub, D. R. *J. Chem. Phys.* **1998**, *108*, 4439.

(40) (a) Foresman, J. B.; Head-Gordon, M.; Pople, J. A.; Frisch, M. J. *J. Phys. Chem.* **1992**, *96*, 135. (b) Foresman, J. B.; Schlegel, H. B. In *Recent Experimental and Computational Advances in Molecular Spectroscopy*; Gausto, R., Hollas, J. M., Eds.; Kluwer Academic: Dordrecht, The Netherlands, 1993; Vol. 406, p 11. (c) Halls, M. D.; Schlegel, H. B. *Chem. Mater.* **2001**, *13*, 2632. (d) Tirapattur, S.; Belletête, M.; Leclerc, M.; Durocher, G. *THEOCHEM* **2003**, *625*, 141. (e) Yang, L.; Feng, J. K.; Ren, A. M. *J. Comput. Chem.* **2005**, *26*, 969.

(41) Hariharan, P. C.; Pople, J. A. *Mol. Phys.* **1974**, *27*, 209.

(42) Gordon, M. S. *Chem. Phys. Lett.* **1980**, *76*, 163.

(43) Lee, C.; Yang, W.; Parr, R. G. *Phys. Rev. B* **1988**, *37*, 785.

(44) Becke, A. D. *Phys. Rev. A* **1988**, *38*, 3098.

(45) Perdew, J. P. *Phys. Rev. B* **1986**, *33*, 8822.

(46) Perdew, J. P.; Chevary, J. A.; Vosko, S. H.; Jackson, K. A.; Pederson, M. R.; Singh, D. J.; Fiolhais, C. *Phys. Rev. B* **1992**, *46*, 6671.

(47) Stephens, P. J.; Devlin, F. J.; Chabalowski, C. F.; Frisch, M. J. *J. Phys. Chem.* **1994**, *98*, 11623.

(48) Becke, A. D. *J. Chem. Phys.* **1993**, *98*, 5648.

(49) Becke, A. D. *J. Chem. Phys.* **1992**, *96*, 2155.

(50) Becke, A. D. *J. Chem. Phys.* **1992**, *97*, 9173.

(51) Perdew, J. P.; Wang, Y. *Phys. Rev. B* **1992**, *45*, 13244.

(52) (a) Hohenberg, P.; Kohn, W. *Phys. Rev.* **1964**, *136*, B864. (b) Kohn, W.; Sham, L. J. *Phys. Rev.* **1965**, *140*, A1133. (c) Slater, J. C. In *Quantum Theory of Molecules and Solids. Vol. 4: The Self-Consistent Field for Molecular and Solids*; McGraw-Hill: New York, 1974.

(53) Vosko, S. H.; Wilk, L.; Nusair, M. *Can. J. Phys.* **1980**, *58*, 1200.

(54) Frisch, M. J.; Pople, J. A.; Binkley, J. S. *J. Chem. Phys.* **1984**, *80*, 3265.

(55) Dunning, T. H., Jr.; Hay, P. J. In *Modern Theoretical Chemistry*; Schaefer, H. F., III, Ed.; Plenum: New York, 1976, pp 1−28.

(56) Reed, A. E.; Curtiss, L. A.; Weinhold, F. *Chem. Rev.* **1988**, *88*, 899.

(57) Frisch, M. J.; Trucks, G. W.; Schlegel, H. B.; Scuseria, G. E.; Robb, M. A.; Cheeseman, J. R.; Zakrzewski, V. G.; Montgomery, J. A., Jr.; Stratmann, R. E.; Burant, J. C.; Dapprich, S.; Millam, J. M.; Daniels, A. D.; Kudin, K. N.; Strain, M. C.; Farkas, O.; Tomasi, J.; Barone, V.; Cossi, M.; Cammi, R.; Mennucci, B.; Pomelli, C.; Adamo, C.; Clifford, S.; Ochterski, J.; Petersson, G. A.; Ayala, P. Y.; Cui, Q.; Morokuma, K.; Malick, D. K.; Rabuck, A. D.; Raghavachari, K.; Foresman, J. B.; Cioslowski, J.; Ortiz, J. V.; Stefanov, B. B.; Liu, G.; Liashenko, A.; Piskorz, P.; Komaromi, I.; Gomperts, R.; Martin, R. L.; Fox, D. J.; Keith, T.; Al-Laham, M. A.; Peng, C. Y.; Nanayakkara, A.; Gonzalez, C.; Challacombe, M.; Gill, P. M. W.; Johnson, B. G.; Chen, W.; Wong, M. W.; Andres, J. L.; Head-Gordon, M.; Replogle, E. S.; Pople, J. A. *Gaussian 98*, revision A.9; Gaussian, Inc.: Pittsburgh, PA, 1998.

(58) Frisch, M. J.; Trucks, G. W.; Schlegel, H. B.; Scuseria, G. E.; Robb, M. A.; Cheeseman, J. R.; Montgomery, J. A., Jr.; Vreven, T.; Kudin, K. N.; Burant, J. C.; Millam, J. M.; Iyengar, S. S.; Tomasi, J.; Barone, V.; Mennucci, B.; Cossi, M.; Scalmani, G.; Rega, N.; Petersson, G. A.; Nakatsuji, H.; Hada, M.; Ehara, M.; Toyota, K.; Fukuda, R.; Hasegawa, J.; Ishida, M.; Nakajima, T.; Honda, Y.; Kitao, O.; Nakai, H.; Klene, M.; Li, X.; Knox, J. E.; Hratchian, H. P.; Cross, J. B.; Adamo, C.; Jaramillo, J.; Gomperts, R.; Stratmann, R. E.; Yazyev, O.; Austin, A. J.; Cammi, R.; Pomelli, C.; Ochterski, J. W.; Ayala, P. Y.; Morokuma, K.; Voth, G. A.; Salvador, P.; Dannenberg, J. J.; Zakrzewski, V. G.; Dapprich, S.; Daniels, A. D.; Strain, M. C.; Farkas, O.; Malick, D. K.; Rabuck, A. D.; Raghavachari, K.; Foresman, J. B.; Ortiz, J. V.; Cui, Q.; Baboul, A. G.; Clifford, S.; Cioslowski, J.; Stefanov, B. B.; Liu, G.; Liashenko, A.; Piskorz, P.; Komaromi, I.; Martin, R. L.; Fox, D. J.; Keith, T.; Al-Laham, M. A.; Peng, C. Y.; Nanayakkara, A.; Challacombe, M.; Gill, P. M. W.; Johnson, B.; Chen, W.; Wong, M. W.; Gonzalez, C.; and Pople, J. A. *Gaussian 03*, revision B.03; Gaussian, Inc., Pittsburgh, PA, 2003.

(59) Bondi, A. *J. Phys. Chem.* **1964**, *68*, 441.